Security-Aware Resource Allocation with Delay Constraint for NOMA-based Cognitive Radio Network

Lei Xu *IEEE Member*, A. Nallanathan *IEEE Fellow*, Xiaofei Pan, and Wenhe Liao

***Abstract*—In this paper, a downlink security-aware resource allocation problem with delay constraint via spectrum sensing is modeled as a mixed integer non-linear problem (MINLP) for non-orthogonal multiple access (NOMA)-based cognitive radio network. The security-aware resource allocation is subject to constraints in required delay for each secondary user, maximum number of accessed secondary users at each subchannel, total interference power threshold introduced to primary user, and total power consumption at secondary BS. The security-aware resource allocation is based on channel state information (CSI) at the physical layer and queue state information (QSI) at the link layer. In order to determine the secrecy transmission rate of each secondary user according to the queue buffer occupancy, a probability upper bound of exceeding the maximum packet delay based on M/D/1 queueing model is analyzed in terms of a required minimum secrecy transmission rate. Then, security-aware secondary user scheduling and power allocation sub-problems are solved, separately. Finally, the secondary user scheduling problem is solved via greedy algorithm, and a power allocation algorithm is proposed by successive convex approximation (SCA) method. The simulation results demonstrate that the performance of proposed algorithms can be improved significantly.**

***Index Terms*—NOMA-based cognitive radio network, security-aware resource allocation, packet delay, successive convex approximation.**

I. Introduction

NOn-orthogonal multiple access (NOMA) technique is widely considered as one of the promising techniques to improve the system capacity of future wireless communication networks [1], [2]. In particular, NOMA uses the power domain for multiple access, where different users are served at different power levels [3]. In NOMA, the users employ successive interference cancelation (SIC) to remove the messages intended for other users before decoding their own messages [4]. On the other hand, combining NOMA and orthogonal frequency division multiplexing (OFDM) can further enhance the spectral efficiency as well as accommodate more users compared to conventional frequency division multiple access (OFDMA) systems. Since the spectrum resources are not utilized efficiently, cognitive radio can be applied in NOMA-based wireless network via accessing the licensed spectrum opportunistically to improve the spectrum efficiency further. In this work, we investigate the resource allocation problem for NOMA-based cognitive radio network.

To utilize the spectrum resource of NOMA-based radio network efficiently, radio resource management is needed. The resource allocation algorithms for NOMA-based radio network can be divided into three categories, i.e., power allocation algorithms [5]–[7], joint power allocation and user scheduling algorithms [8]–[10], and resource allocation algorithm based on energy harvesting [11]–[13]. Tailored for the power allocation, a joint power allocation algorithm is designed for NOMA-based amplify-and-forward relay network to maximize achievable transmission rate at the destination with quality of service (QoS) constraints, i.e., achievable transmission rate constraints at other destinations and individual transmission power constraints [5]. In [6], a suboptimal power allocation algorithm is designed for downlink NOMA-based radio network with delay QoS constraint. In [7], the NOMA-based radio network with a linear multiuser superposition transmission scheme is investigated, and a power allocation algorithm is proposed via maximizing the total mutual information.

In order to improve the network performance further, the joint power allocation and user scheduling algorithms are designed in [8]–[10]. A joint sub-channel assignment, user scheduling, and power allocation for NOMA-based radio network is presented via a many-to-many two-sided matching game to maximize the weighted sum-rate, while taking into account user fairness [8]. In [9], a

Lei Xu and Xiaofei Pan are at the School of Computer Science and Engineering, Nanjing University of Science and Technology, Nanjing, China. Wenhe Liao at with the School of Mechanical Engineering, Nanjing University of Science and Technology, Nanjing, China. (E-mail: xulei_marcus@126.com).

A. Nallanathan is at the Department of Informatics, King's College London, London WC2R 2LS, U.K. (E-mail: nallanathan@ieee.org).

joint power allocation and user scheduling algorithm for NOMA-based radio network is proposed via Lagrangian duality and dynamic programming methods. In [10], two joint power allocation and user scheduling algorithms for multicarrier NOMA-based radio network is designed with a full-duplex base station for serving multiple half-duplex downlink and uplink users.

For NOMA-based radio network, a wireless-powered uplink communication system is designed consisting one base station and multiple energy harvesting users, and an efficient greedy algorithm is proposed to improve the individual transmission rate and user fairness [11]. In [12], the durations of the energy harvesting and information transmission phases are designed for the uplink NOMA-based radio network. In [13], a joint optimal rate and time allocation with proportional fairness is proposed for uplink NOMA-based radio network.

Although the joint user scheduling and power allocation problems are investigated for NOMA-based radio network in [8]–[10], how cognitive radio technology affects the security-aware resource allocation problem for NOMA-based radio network needs further studies. In this paper, we study the security-aware resource allocation with delay constraint for NOMA-based cognitive radio network. The contributions of this work is summarized as follows: (i) We formulate a downlink security-aware resource allocation problem based on delay constraint as an MINLP model to schedule the secondary users at each subchannel and allocate the power among different secondary users with CSI and QSI; (ii) A probability upper bound of exceeding the maximum packet delay is analyzed in terms of a required secrecy transmission rate according to M/D/1 queueing model; (iii) A secondary user scheduling algorithm is designed with the greedy algorithm, and a power allocation algorithm is proposed based on the SCA method.

The rest of this paper is organized as follows. System model is described in Sections II. Section III presents the security-aware resource allocation problem formulation with delay constraint. The security-aware resource allocation algorithm with delay constraint is given in Section IV. Finally, performance evaluation and conclusions are given in Sections V and VI, respectively.

II. System Model

In this section, we first describe the system of NOMA-based cognitive radio network. Then, interference power model is given. Finally, secrecy transmission rate model is proposed.

A. System Description

Consider a geographical area with a primary network and a cognitive network [14], as shown in Fig. 1. The physical layer in primary network and cognitive network adopts NOMA technology. There is an eavesdropper in NOMA-based cognitive radio network. The eavesdropper is passive and aims to wiretap the transmitted signal in all the data-bearing subchannels[1]. Additionally, the wireless channels between secondary users and secondary BS or the eavesdropper are assumed to be perfectly known [17]. At NOMA-based primary network, there exists a set, $\mathcal{N}=\{1,2,\cdots,N\}$, of primary users. Additionally, for NOMA-based cognitive radio network, there are a set, $\mathcal{M}=\{1,2,\cdots,M\}$, of secondary users. At the physical layer, the bandwidth is divided into orthogonal subchannels for NOMA-based primary network, and NOMA technology is adopted at each subchannel. Additionally, secondary users in NOMA-based cognitive radio network access the vacant subchannels opportunistically. The set of subchannels for NOMA-based primary network is $\mathcal{K}^v=\{1,2,\cdots,K^v\}$. In order to protect the communication for primary NOMA network, the transmission power at secondary BS should be limited, and the interference temperature model is adopted [18]. At NOMA-based cognitive radio network, secondary user with the near distance to secondary BS is allocated with smaller power, and secondary user with the far distance to secondary BS is allocated with larger power. With the normalized channel gain with the interference and noise power, successive interference cancellation is adopted at secondary users' receiver [19]. Via a reliable common control channel, the spectrum sensing information and security-aware resource allocation results are exchanged between secondary BS and secondary users.

At secondary BS and each secondary user, they are both equipped with one antenna. At secondary BS, a subset of secondary users is scheduled at each subchannel owing to the NOMA technology, and power is allocated among secondary users. Time is partitioned into time slots, $\mathcal{T}=\{1,2,\cdots\}$, of equal duration τ. It is assumed that the channel power gains remain constant within one time slot, and vary from one time slot to another time slot and from one link to another link, independently. The resource allocation is performed at the beginning of each time slot, remains constant within one time slot and varies from one time slot to another time slot. At subchannel k, the subset of active secondary users is $\mathcal{S}_k$.

[1]For secure transmission, information-theoretic security is built by Shannon's information theory, and the concept of wiretap channel is proposed in [15], [16].

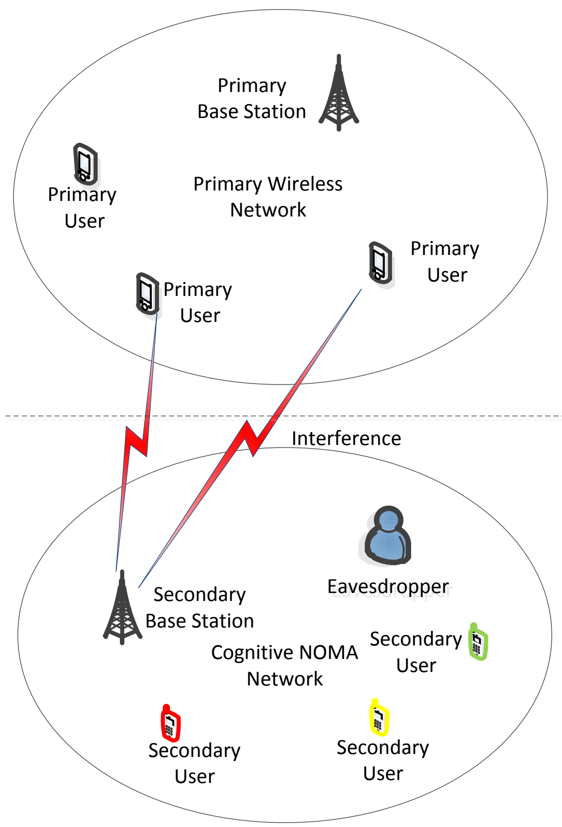

Fig. 1. NOMA-based cognitive radio network.

At subchannel k, q_u secondary users at most can share one subchannel in each time slot, and secondary user, $m \in \mathcal{S}_k$, generates the interference to other secondary users with the same subchannel. The signal for secondary user m at subchannel k is

$$y_m^k = g_m^k \sum_{\overline{m} \in S_k} \sqrt{P_{\overline{m}}^k} x_{\overline{m}}^k + n_m^k \tag{1}$$

where n_m^k is the additive white Gaussian noise for secondary user m at the subchannel k, $x_{\overline{m}}^k$ is the transmission symbol for secondary user $\overline{m}$ at subchannel k, g_m^k is the channel power gain for secondary user m at subchannel k, and $P_{\overline{m}}^k$ is the allocated power for secondary user $\overline{m}$ at subchannel k.

B. Interference Power Model

Define the bandwidth of each subchannel as B, and the spectrum bandwidth of subchannel j spans from $f_s + (j-1)B$ to $f_s + jB$. When the secondary BS communicates with the unit transmission power over the subchannel k to secondary user m, the interference power, I_{mn}^{kj}, introduced to the subchannel j for primary user n, is [20]

$$I_{mn}^{kj} = \int_{(j-1)B-(k-0.5)B}^{jB-(k-0.5)B} h_n^k \phi(f) df \tag{2}$$

where h_n^k is the channel power gain between secondary BS and primary user n over subchannel k, and $\phi(f)$ is the power spectrum density for each NOMA signal, i.e.,[2],

$$\phi(f) = T \left(\frac{\sin \pi f T}{\pi f T} \right)^2 \tag{3}$$

where T is the symbol duration.

C. Secrecy Transmission Rate Model

The secrecy transmission rate for secondary BS to communicate with secondary user m at subchannel k is

$$R_m^k = \begin{cases} B \log_2 \left(\frac{Bn_0 + IF_k^S + IO_{mk}^S + P_m^k g_m^k}{Bn_0 + IF_k^E + IO_{mk}^E + P_m^k f_e^k} \right), g_m^k \geq f_e^k \\ 0, g_m^k < f_e^k \end{cases} \tag{4}$$

where P_m^k is the power allocated to subchannel k for secondary user m, IF_k^S is the interference power introduced to secondary BS from primary network at subchannel k, IF_k^E is the interference power introduced to eavesdropper from primary network at subchannel k[3], and n_0 is one-sided noise power spectral density. Additionally, the channel gain at subchannel k between the eavesdropper and secondary BS is f_e^k. The interference power, IO_{mk}^S, for secondary user m introduced by the other secondary users at the same subchannel k is

$$IO_{mk}^S = \sum\nolimits_{l \in \left\{ \mathcal{M}^* \middle| \frac{g_l^k}{Bn_0} > \frac{g_m^k}{Bn_0} \right\}} P_l^k g_m^k. \tag{5}$$

Additionally, the interference power, IO_{mk}^E, for eavesdropper introduced by the other secondary users at the same subchannel k is

$$IO_{mk}^E = \sum\nolimits_{l \in \left\{ \mathcal{M}^* \middle| \frac{g_l^k}{Bn_0} > \frac{g_m^k}{Bn_0} \right\}} P_l^k f_e^k. \tag{6}$$

Define the lower bound of secrecy transmission rate $\overline{R}_m^k$. Since $IO_{mk}^S \geq IO_{mk}^E$ and $IF_k^S \geq IF_k^E$, $R_m^k \geq \overline{R}_m^k$.

$$\overline{R}_m^k = B \log_2 \left(\frac{Bn_0 + IF_k^S + IO_{mk}^S + P_m^k g_m^k}{Bn_0 + IF_k^S + IO_{mk}^S + P_m^k f_e^k} \right). \tag{7}$$

[2]In this work, assume that the CSI from the primary BS to the secondary users is perfect known, and the CSI from the secondary BS to the primary users is also perfect known. This assumption is used for resource allocation in cognitive OFDM network, e.g., [21].

[3]In this work, assume $IF_k^S \geq IF_k^E$, which can make the later analysis conveniently.

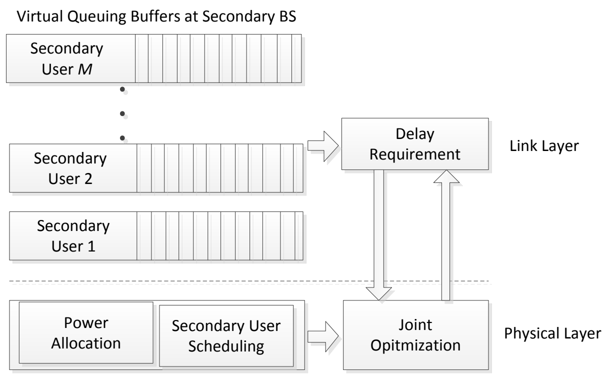

Fig. 2. Cross-layer resource allocation design.

III. Security-Aware Resource Allocation Problem Formulation

In this section, we first describe the cross-layer resource allocation design. Then, the packet delay analysis is given. Finally, we formulate the security-aware resource allocation problem.

A. Cross-Layer Resource Allocation Design

At secondary BS, each secondary user has a virtual queueing buffer, and the buffer size for each secondary user is infinite. Each secondary user has a video packet flow to transmit via secondary BS. In order to improve the coding efficiency of multiview video coding, variable block-size motion estimation, disparity estimation, and multiple reference frames selection are adopted [22]–[24]. Additionally, each packet should be transmitted before a deadline. If the transmission delay exceeds the bound, the packet is dropped from its queueing buffer. Fig. 2 shows the cross-layer resource allocation design for NOMA-based cognitive radio network. Resource allocation at the physical layer and the queueing buffer for each secondary user at the link layer are considered in this work. Based on the occupancy at the the queueing buffer and the packet delay requirement for video traffic, the required minimum secrecy transmission rate at the physical layer is analyzed for each secondary user. On the other hand, the performance of the packet delay at the link layer is influenced by the practical physical secrecy transmission rate. Consequently, designing the secondary user scheduling and power allocation at the physical layer is necessary to incorporate the delay requirement information at the link layer.

B. Packet delay Analysis

Assume that the video packet arrivals at the transmission buffer of secondary user m follow a Poisson process [14]. The average arrival rate is λ_m, and the constant packet length is L bits [19]. Since the service rate of the packet at secondary user m is defined as the transmission rate R_m[4], the service time for each packet of each secondary user is deterministic. Consequently, the packet buffer is modeled as an M/D/1 queuing system[5]. For the stability of the queue, we have

$$\rho_m = \lambda_m L / R_m < 1. \tag{8}$$

At the queueing system, $\pi = (\pi_0, \pi_1, \cdots)$ is the stationary distribution of the number of packets. According to Pollaczek-Khinchin formula [25], the probability generating function, $\pi(z)$, is

$$\pi(z) = \frac{(1-\rho_m)(1-z)\,\mathrm{e}^{\rho_m(z-1)}}{\mathrm{e}^{\rho_m(z-1)} - z}. \tag{9}$$

The stationary probability, π_i, is given by (7) with Taylor expansion of $\pi(z)$ [26].

$$\begin{aligned}
&\pi_0 = 1 - \rho_m \\
&\pi_1 = (1-\rho_m)\left(e^{\rho_m} - 1\right) \\
&\pi_i = (1-\rho_m)\left(e^{i\rho_m} + \varpi_i\right), i \geq 2 \\
&\varpi_i = \sum_{j=1}^{i-1} e^{j\rho_m} (-1)^{i-j} \left[\frac{(j\rho_m)^{i-j}}{(i-j)!} + \frac{(j\rho_m)^{i-j-1}}{(i-j-1)!}\right].
\end{aligned} \tag{10}$$

Given the packet length and service rate, the service time for all packets in the M/D/1 queueing system is the same. Consequently, the upper bound for the number of packets in the queue buffer to meet the maximum delay requirement is

$$Q_m^{\max} = \lfloor D_m^{\max} R_m / L \rfloor \tag{11}$$

where $\lfloor \bullet \rfloor$ is the floor function.

For each new packet arrival, the packet delay is the ratio of the number of packets at the queueing system to the service rate[6]. Hence, we have

$$\Pr\left(Q_m > Q_m^{\max}\right) = \Pr\left(D_m > D_m^{\max}\right) \tag{12}$$

[4] R_m is the secrecy transmission rate for secondary user m, while $\overline{R}_m^k$ is the secrecy transmission rate for secondary user m at the subchannel k, i.e., $R_m = \sum\limits_{k \in \mathcal{K}^v} \overline{R}_m^k$.

[5] The video packet arrivals at secondary user m follow a Poisson process, and the service time is determined, and only one single server serves secondary user m. Hence, M/D/1 queueing model is adopted in this work.

[6] Assume the transmission rate is determined. Additionally, the packet delay is proportional fairness to the number of packets at the queueing system. Therefore, the probability of exceeding the packet delay threshold for the packet delay is equal to that of exceeding the number threshold of packets for the number of packets.

and

$$\Pr\left(Q_m > Q_m^{\max}\right) = 1 - \sum_{i=0}^{Q_m^{\max}} \pi_i \tag{13}$$

where Q_m is the number of packets at the queueing system for secondary user m, D_m is the time of a packet from its generation to its transmission, and $D_m^{\max}$ is the maximum packet delay after which the packet will be dropped at the transmitter.

From (11)-(12), (13) can be rewritten as

$$1 - \sum_{i=0}^{Q_m^{\max}} \pi_i \leq \chi_m. \tag{14}$$

where χ_m is the probability upper bound of exceeding the maximal packet delay.

From (10) and (14), we can obtain the minimum secrecy transmission rate, $\psi\left(D_m^{\max}, \chi_m, \lambda_m, L\right)$, as a function of the delay requirement, the packet average arrival rate, and the packet length, by the binary search method[7]. The secrecy transmission rate for secondary user m should be at least the required minimum secrecy transmission rate in order to satisfy the packet delay requirement, i.e.,

$$\sum_{k\in\mathcal{K}^v} \alpha_m^k \overline{R}_m^k \geq \psi\left(D_m^{\max}, \chi_m, \lambda_m, L\right). \tag{15}$$

where $\alpha_m^k \in \{0,1\}$ is the subchannel allocation indicator for secondary user m at subchannel k. If $\alpha_m^k = 1$, secondary user m uses the subchannel k. Additionally, $\overline{R}_m^k$ is a function of power P_m^k.

C. Security-Aware Resource Allocation Formulation

The power consumption for each secondary user consists of two components [28]. The first component is a fixed power consumption, P_c. The second component refers to the transmission power consumption. In NOMA-based cognitive radio network, the total power consumption at secondary BS should satisfy the maximum available power constraint, i.e.,

$$P_c + \sum_{m\in\mathcal{M}} \sum_{k\in\mathcal{K}^v} \alpha_m^k P_m^k \leq P^{\text{total}} \tag{16}$$

where P^{total} denote the maximum available power at secondary BS.

The packet delay for secondary user m should probabilistically satisfy the maximum packet delay constraint, given by

$$\Pr\left(D_m > D_m^{\max}\right) \leq \chi_m. \tag{17}$$

In order to guarantee the feasible region of subchannel allocation, we add the constraint, i.e.,

$$\sum_{m\in\mathcal{M}} \alpha_m^k \leq q_u, k \in \mathcal{K}^v. \tag{18}$$

The interference power at primary user n should satisfy the constraint, i.e.,

$$\sum_{m\in\mathcal{M}} \sum_{k\neq j\in\mathcal{K}^v} \sum_{j\in\mathcal{K}^v} \alpha_m^k P_m^k I_{mn}^{kj} \leq I_n^{\text{th}}, \forall n \in \mathcal{N} \tag{19}$$

where I_n^{th} is the interference threshold for primary user n [29].

The NOMA-based cognitive radio network performance can be evaluated by the total secrecy throughput, and our objective is to maximize the total secrecy throughput subject to the total available power at secondary BS, the required secrecy transmission rate for each secondary user, the interference power constraint, and the maximum number of scheduled secondary users at each subchannel. Consequently, the security-aware resource allocation problem is

$$\begin{aligned} OP1 : &\max_{\alpha_m^k, P_m^k} \sum_{m\in\mathcal{M}} \sum_{k\in\mathcal{K}^v} \alpha_m^k \overline{R}_m^k \\ S.t. :&(15), (16), (18), (19) \\ &\alpha_m^k \in \{0,1\}, P_m^k \geq 0. \end{aligned} \tag{20}$$

where (20) is an MINLP, which is difficult to solve owing to combining the integer variables with the non-linear functions. Consequently, the original security-aware resource allocation problem can be divided into the secondary user scheduling subproblem and the power allocation subproblem, i.e., the integer programming problem and the continuous variable non-linear programming problem.

IV. Security-Aware Resource Allocation Algorithm with Delay Constraint

In this section, the secondary user scheduling algorithm is proposed with the greedy algorithm firstly. Then, the power allocation algorithm is designed via the SCA method. Finally, the computational complexity is analyzed for the proposed algorithms.

[7]The binary search is also known as half-interval search [27]. In the binary search method, there is over a range $\left[R_m^{\min}, R_m^{\max}\right]$, where $R_m^{\min}$ and $R_m^{\max}$ are the search lower and upper bounds for MT m, e.g., $R_m^{\min} = \lambda_m L$ and $R_m^{\max} = 10\lambda_m L$.

A. Secondary User Scheduling Algorithm

The secondary user scheduling problem for NOMA-based cognitive radio network is formulated as

$$\begin{aligned} &OP2:\max_{\alpha_m^k} \sum_{m\in\mathcal{M}}\sum_{k\in\mathcal{K}^v} \alpha_m^k \overline{R}_m^k \\ &S.t.:(18),(19),\alpha_m^k\in\{0,1\}\,. \end{aligned} \tag{21}$$

Problem (21) is a binary integer programming, and a heuristic algorithm for secondary user scheduling based on the greedy algorithm is proposed in algorithm 1. The heuristic algorithm for secondary user scheduling is implemented in secondary BS. Assume the total available power is allocated equally across different available vacant subchannels among different secondary users. The secondary user is selected with the fairness criterion, and the subchannel is selected with the largest interference power margin for the tagged secondary user. If there is idle interference power margin available at the primary user, secondary BS allows secondary users to utilize the vacant subchannel. The secrecy transmission rate set for all secondary users and the secrecy transmission rate set for each secondary user at each subchannel are defined by $\mathcal{SR}$ and $\mathcal{R}=\left\{\overline{R}_m^k\right\}$, respectively. Firstly, secondary BS senses the vacant subchannels. Secondly, secondary BS selects the secondary user with the minimum secrecy transmission rate. Then, the tagged secondary user selects an available vacant subchannel with the largest secrecy transmission rate, and updates the interference power at the primary users. Finally, if primary users can afford the interference power for the new assigned secondary user and vacant subchannel pair, assign it; otherwise, stop and terminate this algorithm. $\mathcal{NK}^v$ is the temporary vacant subchannel set. Since the secondary user scheduling algorithm is designed via greedy algorithm, the convergence can be guaranteed [30].

Algorithm 1 Secondary User Scheduling Algorithm.

Input: P^{total}, $D_m^{\max}$, χ_m, λ_m, L, q_u, and I_n^{th}.
Output: α_m^k.

1: Initialize $\alpha_m^k=0$, P_m^k, $\mathcal{SR}$, $\mathcal{R}$, and I_m^k.
2: **repeat**
3: Select the secondary user, $m^*=\min_{m\in\mathcal{M}}\mathcal{SR}$.
4: Select the subchannel, $k^*=\max_{k\in\mathcal{NK}^v}\overline{R}_{m^*}^k$, for secondary user m^*.
5: Update the interference power $I_{m^*}^{k^*}$, $\mathcal{SR}$, and $\mathcal{R}$.
6: **if** $\sum_{m\in\mathcal{M}}\alpha_m^{k^*}<q_u$ **then**
7: Set $\alpha_{m^*}^{k^*}=1$.
8: **else**
9: Delete the subchannel k^* from the set $\mathcal{NK}^v$.
10: **end if**
11: **if** $\sum_{m\in\mathcal{M}}\sum_{k\in\mathcal{K}^v}\alpha_m^k I_m^k<I_n^{\text{th}}$ **then**
12: Go to Step 3.
13: **else**
14: Stop and output α_m^k.
15: **end if**
16: **until**

B. Power Allocation Algorithm

The power allocation is adjusted based on CSI and QSI, to maximize the secrecy throughput of NOMA-based cognitive radio network, while satisfying the secondary BS available power limitation, the available vacant subchannel resources, the required minimum secrecy transmission rate, and the interference power constraint at each primary user, i.e.,

$$\begin{aligned} &OP3:\max_{P_m^k} \sum_{m\in\mathcal{M}}\sum_{k\in\mathcal{K}^v} \alpha_m^k \overline{R}_m^k \\ &S.t.:(13),(14),(17),P_m^k\geq 0. \end{aligned} \tag{22}$$

where (22) is a non-convex optimization problem, and it is hard to find an accurate solution to the nonconvex optimization problem. However, we can utilize the SCA method to approximate the objective function into a series of convex functions.

According to [31], a lower bound of $\overline{R}_m^k$ is

$$\begin{aligned} \overline{R}_m^k &= \alpha_m^k B\log_2\left(1+\gamma_m^k\right) \\ &\geq \alpha_m^k B\left[b_{mk}\log_2\left(\gamma_m^k\right)+c_{mk}\right] \end{aligned} \tag{23}$$

and

$$\gamma_m^k=\frac{P_m^k\left(g_m^k-f_e^k\right)}{Bn_0+IF_k^S+IO_{mk}^S+P_m^k f_e^k}. \tag{24}$$

The approximation is equal to the exact one when

$$b_{mk}=\frac{\gamma_m^k}{1+\gamma_m^k} \tag{25}$$

and

$$c_{mk}=\log_2\left(1+\gamma_m^k\right)-\frac{\gamma_m^k}{1+\gamma_m^k}\log_2\left(\gamma_m^k\right). \tag{26}$$

For given approximation coefficients $\mathcal{B}\triangleq\{b_{mk}\}$ and $\mathcal{C}\triangleq\{c_{mk}\}$, the objective function in (22) is still non-concave. However, we can further introduce the transformation of $\overline{P}_m^k=\ln P_m^k$. Hence, the original problem (22) can be converted into

$$\begin{aligned}
&OP4:\max_{\overline{P}_m^k}\sum_{m\in\mathcal{M}}\sum_{k\in\mathcal{K}^v}\alpha_m^k B\left(b_{mk}\log_2\gamma_m^k+c_{mk}\right)\\
&S.t.:C1.P_c+\sum_{m\in\mathcal{M}}\sum_{k\in\mathcal{K}^v}\alpha_m^k\exp\left(\overline{P}_m^k\right)\le P^{\text{total}}\\
&\quad C2.\sum_{k\in\mathcal{K}^v}\alpha_m^k B\left(b_{mk}\log_2\gamma_m^k+c_{mk}\right)\ge\\
&\quad\psi\left(D_m^{\max},\chi_m,\lambda_m,L\right),\forall m\in\mathcal{M}\\
&\quad C3.\sum_{m\in\mathcal{M}}\sum_{k\in\mathcal{K}^v}\alpha_m^k I_{mn}^k\exp\left(\overline{P}_m^k\right)\le I_n^{th}.
\end{aligned}\tag{27}$$

***Proposition** 1:* Problem (27) is a convex optimization problem.

Proof: See Appendix A.

Since problem (27) is a convex optimization problem, it is appropriate to solve (27) via the dual decomposition method [32]. The Lagrangian function for problem (27) is

$$\begin{aligned}
&f\left(v,u_m,\delta_n,\bar{P}_m^k\right)=\\
&\sum_{m\in\mathcal{M}}\sum_{k\in\mathcal{K}^v}\alpha_m^k B\left(b_{mk}\log_2\gamma_m^k+c_{mk}\right)\\
&+v\left\{P^{\text{total}}-\left(P_c+\sum_{m\in\mathcal{M}}\sum_{k\in\mathcal{K}^v}\alpha_m^k\exp\left(\bar{P}_m^k\right)\right)\right\}\\
&+\sum_{n\in\mathcal{N}}\delta_n\left\{I_n^{th}-\sum_{m\in\mathcal{M}}\sum_{k\in\mathcal{K}^v}\alpha_m^k I_{mn}^k\exp\left(\bar{P}_m^k\right)\right\}\\
&+\sum_{m\in\mathcal{M}}u_m\left\{\sum_{k\in\mathcal{K}^v}\alpha_m^k B\left(b_{mk}\log_2\gamma_m^k+c_{mk}\right)\right.\\
&\left.-\psi\left(D_m^{\max},\chi_m,\lambda_m,L\right)\right\}
\end{aligned}\tag{28}$$

where v, u_m, and δ_n are the Lagrangian multipliers.

According to (28), the dual function $h\left(v,u_m,\delta_n\right)$ can be expressed as

$$h\left(v,u_m,\delta_n\right)=\left\{\begin{array}{l}\max\limits_{\overline{P}_m^k}f\left(v,u_m,\delta_n,\overline{P}_m^k\right)\\ S.t.:\overline{P}_m^k\ge 0.\end{array}\right.\tag{29}$$

Additionally, the dual problem is

$$\begin{aligned}
&OP5:\min_{v,u_m,\delta_n}h\left(v,u_m,\delta_n\right)\\
&S.t.:v\ge 0,u_m\ge 0,\delta_n\ge 0.
\end{aligned}\tag{30}$$

The power allocation can be obtained with (44), which is proven in Appendix B. The optimum values v, u_m, and δ_n can be calculated by solving the dual problem (30). For a fixed $\overline{P}_m^k$, the dual problem (30) can be simplified to

$$\begin{aligned}
&\min:v\left\{P^{\text{total}}-\left(P_c+\sum_{m\in\mathcal{M}}\sum_{k\in\mathcal{K}^v}\alpha_m^k\exp\left(\bar{P}_m^k\right)\right)\right\}\\
&+\min:\sum_{n\in\mathcal{N}}\delta_n\left\{I_n^{th}-\sum_{m\in\mathcal{M}}\sum_{k\in\mathcal{K}^v}\alpha_m^k I_{mn}^k\exp\left(\bar{P}_m^k\right)\right\}\\
&+\min:\sum_{m\in\mathcal{M}}u_m\left\{\sum_{k\in\mathcal{K}^v}\alpha_m^k B\left(b_{mk}\log_2\gamma_m^k+c_{mk}\right)\right.\\
&\left.-\psi\left(D_m^{\max},\chi_m,\lambda_m,L\right)\right\}.
\end{aligned}\tag{31}$$

For a differentiable dual function (31), a gradient descent method can be applied to calculate the optimal values for v, u_m , and δ_n, and we can obtain

$$v\left(i+1\right)=\left[v\left(i\right)-\Delta\varepsilon_1\Delta v\right]^+\tag{32}$$

$$\delta_n\left(i+1\right)=\left[\delta_n\left(i\right)-\Delta\varepsilon_2\Delta\delta\right]^+\tag{33}$$

$$u_m\left(i+1\right)=\left[u_m\left(i\right)-\Delta\varepsilon_3\Delta u\right]^+\tag{34}$$

$$\Delta v=P^{\text{total}}-\left(P_c+\sum_{m\in\mathcal{M}}\sum_{k\in\mathcal{K}^v}\alpha_m^k\exp\left(\bar{P}_m^k\right)\right)\tag{35}$$

$$\Delta\delta=I_n^{th}-\sum_{m\in\mathcal{M}}\sum_{k\in\mathcal{K}^v}\alpha_m^k I_{mn}^k\exp\left(\bar{P}_m^k\right)\tag{36}$$

and

$$\begin{aligned}
\Delta u=&\sum_{k\in\mathcal{K}^v}\alpha_m^k B\left(b_{mk}\log_2\gamma_m^k+c_{mk}\right)\\
&-\psi\left(D_m^{\max},\chi_m,\lambda_m,L\right)
\end{aligned}\tag{37}$$

where i is the iteration index and $\Delta\varepsilon_j$, $j=1,2,3$, is a small step size. Since the gradient of problem (31) satisfies the Lipchitz continuity condition, the convergence towards the optimum solution is guaranteed by (32)-(37) with an appropriate step size [32]. Consequently, the power allocation solutions in (44) converges to the optimum solution.

To find the solution of problem (22), we need to further find the tightened bound by iteratively updating $\mathcal{B}$ and $\mathcal{C}$. The process of tightening $\mathcal{B}$ and $\mathcal{C}$ is detailed in algorithm 2. Now, the original problem has been transformed into a series of convex optimizations in (27). Here, we will develop an algorithm to solve the problem in (22), which is an upper bound algorithm for (22) [33]–[35]. In algorithm 2, Δ is the maximum tolerance, I_{max} is the maximum number of iteration, and t is the iteration index. With the logarithmic approximation (23), a sequence of improved feasible solutions is generated via the SCA approach, which will finally converge to a locally optimal solution [31].

Although (44) gives the solution to the power allocation, it still remains to design an algorithm to provide the execution structure and the executing entity of the equations. Consequently, we propose algorithm 3 as an

Algorithm 2 The Process of SCA Algorithm.

Input: P^{total}, $D_m^{\max}$, χ_m, λ_m, L, and I_n^{th}.
Output: b_{mk}^{t+1} and c_{mk}^{t+1}.

1: Initialize $b_{mk}^0 = 1$, Δ, I_{max}, $t = 0$, and $c_{mk}^0 = 0$.
2: **repeat**
3: Obtain the power $\overline{P}_m^k$ with algorithm 3.
4: Update elements of b_{mk}^{t+1} and c_{mk}^{t+1} using (23) and (24).
5: **if** $\left|b_{mk}^{t+1} - b_{mk}^t\right| \leq \Delta$ and $\left|c_{mk}^{t+1} - c_{mk}^t\right| \leq \Delta$ **then**
6: Stop, and output b_{mk}^{t+1} and c_{mk}^{t+1}.
7: **else**
8: Set $t = t + 1$, and go to step 4.
9: **end if**
10: **until**

Algorithm 3 Power Allocation Algorithm.

Input: P^{total}, φ_m, and I_n^{th}.
Output: $\overline{P}_m^k$.

1: Initialize $v(i) \geq 0$, $u_m(i) \geq 0$, $\delta_n(i) \geq 0$ and $i = 1$.
2: **repeat**
3: Calculate $\overline{P}_m^k$ with (30).
4: Update $v(i+1)$, $u_m(i+1)$ and $\delta_n(i+1)$.
5: **if** $\left|P^{\mathrm{total}} - P_c - \sum\limits_{m\in\mathcal{M}} \sum\limits_{k\in\mathcal{K}^v} \alpha_m^k \exp\left(\overline{P}_m^k\right)\right| \leq \varepsilon$ or $\left|I_n^{\mathrm{th}} - \sum\limits_{m\in\mathcal{M}} \sum\limits_{k\in\mathcal{K}^v} \alpha_m^k I_{mn}^k \exp\left(\overline{P}_m^k\right)\right| \leq \varepsilon$ **then**
6: Set $i = i + 1$, and go to step 3.
7: **else**
8: Stop, and output $\overline{P}_m^k$.
9: **end if**
10: **until**

implementation to obtain the power allocation, which is described by algorithm 3. ε is an arbitrarily small positive number. $v(i)$, $u_m(i)$, and $\delta_n(i)$ are the Lagrangian multipliers at the i iteration. $v(i+1)$, $u_m(i+1)$, and $\delta_n(i+1)$ are the Lagrangian multipliers at the $(i+1)$ iteration.

C. Computational Complexity Analysis

In the proposed secondary user scheduling algorithm, the computational complexity is $O(3MK^v q_u)$. In the power allocation algorithm, the computational complexity is in number of dual variables. The computational complexity is given by $O\left(O_I I_{\max} M^2 q_u K^v\right)$, where O_I is the number of iterations required for the convergence and $I_{\max}$ is the number of iterations required for algorithm 2. Consequently, the total computational complexity is $O\left(3MK^v q_u + O_I I_{\max} M^2 q_u K^v\right)$. For the required feedback overhead, secondary BS broadcasts its scheduling information to all secondary users, and the signal overhead is $O(MK^v q_u)$.

V. Performance Evaluation

In this section, we evaluate the performance of security-aware resource allocation for NOMA-based cognitive radio network. Consider a geographical area covered by a primary wireless network and a cognitive wireless network. The radius of cognitive NOMA network is 200 m. The path loss fact is 4. There are two primary users, and the distances between secondary BS and primary users are 300 m and 600 m. There exists an eavesdropper in NOMA-based cognitive radio network, and the distances from the eavesdropper to the secondary BS is 900 m. The average packet arrival rate for each secondary user is $\lambda_m = 2.5 \times 10^3$ packets/s, and the maximum packet delay for secondary user m is $D_m^{\max} = 1$ ms. The probability upper bound of exceeding the maximum packet delay for secondary user m is $\chi_m = 0.01$, and the packet length is $L = 1024$ bits [36]. The noise power is 1×10^{-12} W. The probability of primary user activity at each subchannel is uniform distributed over [0, 1]. The other simulation parameter is $P_c = 20$ dBm. There are three cases for the proposed algorithm, i.e., $q_u = 3$ for NOMA scheme, $q_u = 2$ for NOMA scheme, and $q_u = 1$ for NOMA scheme.

We evaluate the impact of the total available power at secondary BS on the secrecy throughput for NOMA-based cognitive radio network in Fig. 3. The number of secondary users is 6. The interference power threshold is $I_n^{\mathrm{th}} = 1 \times 10^{-9}$ W. The number of subchannels is $K^v = 64$. The available bandwidth for each subchannel have two cases, i.e., $B = 10$ MHz and $B = 15$ MHz. From Fig. 3, we can see that the total secrecy throughput for NOMA-based cognitive radio network increases with the total available power at secondary BS. As the total available power at secondary BS increases, secondary BS tends to allocate more power to secondary users to improve the total secrecy throughput. However, higher modulation mode consumes more power, and power utilization efficiency decreases. Consequently, the growth trend of total secrecy throughput becomes slower as total available power at secondary BS increases. It can be also seen that the total secrecy throughput of NOMA scheme with $q_u = 3$ are much larger than that of NOMA scheme with $q_u = 1$. This is because in the NOMA scheme with $q_u = 1$, one subchannel can be only allocated to one secondary user, and the secondary BS does not take full advantage of the spectrum resource at the power domain.

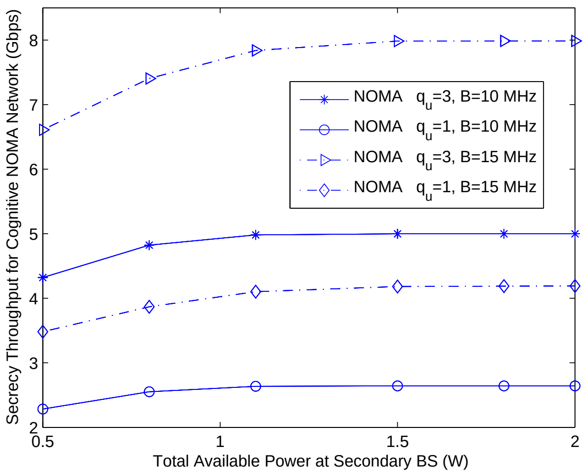

Fig. 3. Total available power at secondary BS vs. secrecy throughput.

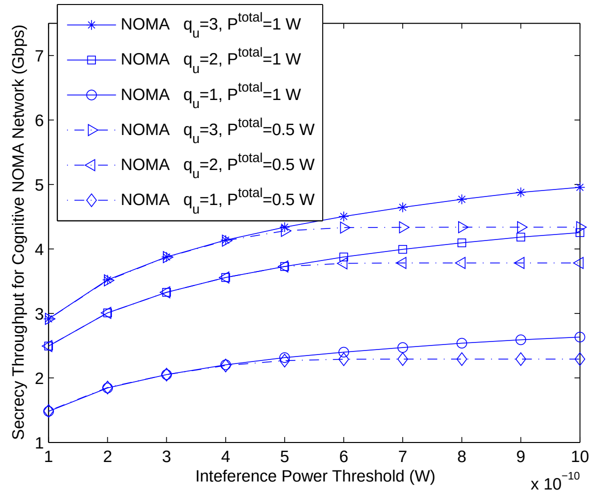

Fig. 4. Interference power threshold vs. secrecy throughput.

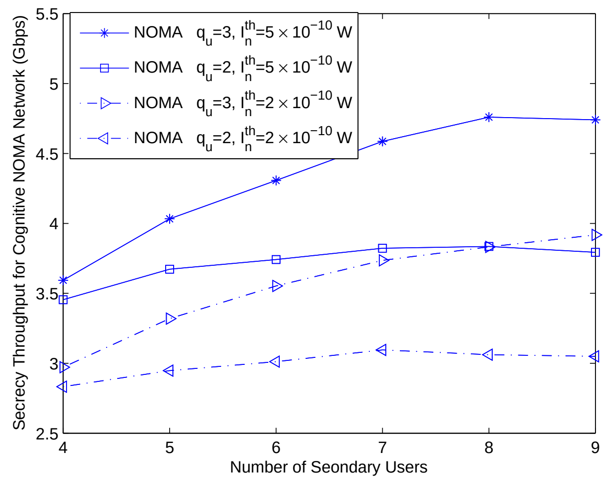

Fig. 5. Number of secondary users vs. secrecy throughput.

We evaluate the impact of the interference power threshold on the secrecy throughput for NOMA-based cognitive radio network in Fig. 4. The number of secondary users is 6. The available bandwidth for each subchannel is $B = 10$ MHz. The number of subchannels is $K^v = 64$. The available power at secondary BS have two cases, i.e., $P^{\text{total}} = 0.5$ W and $P^{\text{total}} = 1$ W. In Fig. 4, it can be seen that the secrecy throughput increases with the interference power threshold. With the case $P^{\text{total}} = 0.5$ W, the secrecy throughput remains unchanged when the interference power threshold exceeds a threshold. This is due to the fact that there is no more power to be allocated for secondary users to improve the secrecy throughput. Additionally, the secrecy throughput with NOMA schemes are larger than that of NOMA scheme with $q_u = 1$. We can also see that the throughput for NOMA scheme with $q_u = 2$ is smaller than that for NOMA scheme with $q_u = 3$. This is due to the fact that NOMA scheme with $q_u = 3$ exploits the power domain more efficiently than NOMA scheme with $q_u = 2$. It obtains the higher spectrum utilization efficiency at the cost of increasing the receiver's complexity.

We evaluate the impact of the number of secondary users on the secrecy throughput for NOMA-based cognitive radio network in Fig. 5. The number of secondary users is 6. T The available bandwidth for each subchannel is $B = 10$ MHz. The number of subchannels is $K^v = 64$. The available power at secondary BS is $P^{\text{total}} = 1$ W. The interference power threshold have two cases, i.e., $I_n^{\text{th}} = 2\times10^{-9}$ W and $I_n^{\text{th}} = 5\times10^{-10}$ W. Fig. 5 shows that the secrecy throughput for NOMA-based cognitive radio network grows with the number of secondary users for NOMA $q_u = 3$ with $I_n^{\text{th}} = 5\times10^{-10}$ W. For NOMA $q_u = 2$, the secrecy throughput for NOMA-based cognitive radio network increases as the number of secondary users increases firstly. Then, it decreases with the number of secondary users. This is because the proposed algorithm with NOMA $q_u = 2$ exploits the power domain diversity at each subchannel firstly. However, the secondary user with the bad channel state information influences the secrecy throughput due to the minimum secrecy transmission rate constraint when the number of secondary users increases. Additionally, we can see that increasing the interference power threshold can improve the secrecy throughput.

We evaluate the impact of the number of the subchannels on the secrecy throughput for NOMA-based cognitive radio network in Fig. 6. The number of secondary users is 4. The available bandwidth for each subchannel is $B = 10$ MHz. The number of subchannels is $K_v = 64$. The interference power threshold is $I_n^{\text{th}} = 5 \times 10^{-10}$ W.

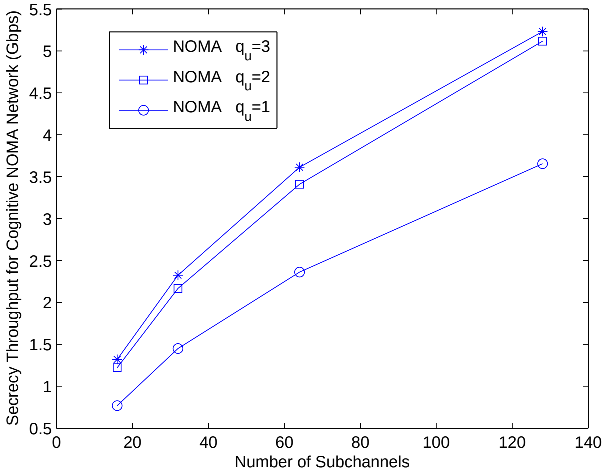

Fig. 6. Number of the subchannels vs. secrecy throughput.

The total power for secondary BS have two cases, i.e., $P^{\text{total}} = 2$ W and $P^{\text{total}} = 4$ W. In Fig. 6, we can see that the secrecy throughput for NOMA-based cognitive radio network increases as the number of subchannels grows. This is due to the fact that increasing the number of subchannel means increasing the available bandwidth. According to the Shannon theory, increasing the available bandwidth improves the network throughput.

From Fig. 3 to Fig. 6, it can be concluded that the proposed algorithms not only guarantee the minimum secrecy transmission rate, but also improve the total secrecy throughput significantly. Although NOMA scheme improves the wireless network performance, it is at the cost of increasing the complexity of receiver. Consequently, designing a proper value for the parameter q_u can achieve the tradeoff between the performance gain and the receiver complexity of secondary user.

VI. Conclusions

In this paper, we study the downlink security-aware resource allocation problem for NOMA-based cognitive radio network. Secondary BS performs the security-aware resource allocation with the delay constraint according to CSI at the physical layer and QSI at the link layer, so as to maximize the secrecy throughput under the QoS constraints. In order to solve the above security-aware resource allocation problem, M/D/1 queueing model is used to analyze the required minimum secrecy transmission rate for each secondary user according to the occupancy of queueing buffer. Then, the greedy algorithm and SCA method are used to design the secondary user scheduling algorithm and the power allocation algorithm, separatively. Simulation results demonstrate that the proposed algorithms not only improve the spectrum efficiency significantly.

Appendix A
Proof of Proposition 1

Proof: Define the objective function and the constraints in (27) as the functions g_1, f_1, f_2, and f_3, i.e.,

$$\left\{\begin{array}{l} g_1 = \sum\limits_{m\in\mathcal{M}}\sum\limits_{k\in\mathcal{K}^v} \alpha_m^k B\left(b_{mk}\log_2\gamma_m^k + c_{mk}\right) \\ f_1 = P^{\text{total}} - \sum\limits_{m\in\mathcal{M}}\left[P_c + \sum\limits_{k\in\mathcal{K}^v}\alpha_m^k \exp\left(\bar{P}_m^k\right)\right] \\ f_2 = I_n^{th} - \sum\limits_{m\in\mathcal{M}}\sum\limits_{k\in\mathcal{K}^v}\alpha_m^k I_{mn}^k \exp\left(\bar{P}_m^k\right) \\ f_3 = \sum\limits_{k\in\mathcal{K}^v}\alpha_m^k B\left(b_{mk}\log_2\gamma_m^k + c_{mk}\right) \\ -\psi\left(D_m^{\max}, \chi_m, \lambda_m, L\right) \end{array}\right. \tag{38}$$

The second derivatives of g_1, f_1, f_2 and f_3 with respective to $\overline{P}_m^k$ are

$$\left\{\begin{array}{c} \frac{\partial^2 g_1}{\partial\left(\bar{P}_m^k\right)^2} = \frac{\alpha_m^k B b_{mk}}{\left(\gamma_m^k\right)^2\ln 2}\left(\frac{\partial^2\gamma_m^k}{\partial\left(\bar{P}_m^k\right)^2} - \left(\frac{\partial\gamma_m^k}{\partial\bar{P}_m^k}\right)^2\right) \le 0 \\ \frac{\partial^2 f_1}{\partial\left(\bar{P}_m^k\right)^2} = -\alpha_m^k\exp\left(\bar{P}_m^k\right) \le 0 \\ \frac{\partial^2 f_2}{\partial\left(\bar{P}_m^k\right)^2} = -\alpha_m^k I_{mn}^k\exp\left(\bar{P}_m^k\right) \le 0 \\ \frac{\partial^2 f_3}{\partial\left(\bar{P}_m^k\right)^2} = \frac{\alpha_m^k B b_{mk}}{\left(\gamma_m^k\right)^2\ln 2}\left(\frac{\partial^2\gamma_m^k}{\partial\left(\bar{P}_m^k\right)^2} - \left(\frac{\partial\gamma_m^k}{\partial\bar{P}_m^k}\right)^2\right) \le 0 \end{array}\right. \tag{39}$$

and

$$\frac{\partial\gamma_m^k}{\partial\bar{P}_m^k} = \frac{\left(g_m^k - f_e^k\right)\left(Bn_0 + IF_k^S + IO_{mk}^S\right)}{\left(Bn_0 + IF_k^S + IO_{mk}^S + \exp\left(\bar{P}_m^k\right)f_e^k\right)^2} \tag{40}$$

and

$$\frac{\partial^2\gamma_m^k}{\partial\left(\bar{P}_m^k\right)^2} = \frac{-2\left(g_m^k - f_e^k\right)\left(Bn_0 + IF_k^S + IO_{mk}^S\right)f_e^k}{\left(Bn_0 + IF_k^S + IO_{mk}^S + \exp\left(\bar{P}_m^k\right)f_e^k\right)^3}. \tag{41}$$

From (39), the objective function is concave on $\overline{P}_m^k$, and the constraints are concave. Hence, (27) is a convex programming problem.

Appendix B
Proof of Proposition 2

Proof: The optimal power allocation $\overline{P}_m^k$ for the fixed values v, u_m, and δ_n can be calculated with (42) by applying KKT condition on (28) .

$$\frac{\partial f\left(v, u_m, \delta_n, \overline{P}_m^k\right)}{\partial\overline{P}_m^k} = 0. \tag{42}$$

From (42), we can obtain

$$\begin{array}{l} \frac{\alpha_m^k B b_{mk}}{\gamma_m^k\ln 2}\frac{\partial\gamma_m^k}{\partial\overline{P}_m^k} - \delta_n\alpha_m^k I_{mn}^k\exp\left(\overline{P}_m^k\right) \\ -v\alpha_m^k\exp\left(\overline{P}_m^k\right) + \mu_m\frac{\alpha_m^k B b_{mk}}{\gamma_m^k\ln 2}\frac{\partial\gamma_m^k}{\partial\overline{P}_m^k} = 0 \end{array} \tag{43}$$

and

$$\bar{P}_m^k = \left[g_P^*\left(\alpha_m^k, v, u_m, \delta_n\right)\right]^+ \tag{44}$$

where $[\bullet]^+$ is a projection on the positive orthant to account for $\bar{P}_m^k$, and $g_P^*(\bullet)$ is a mapping function which satisfies (42).

Acknowledgments

The authors gratefully acknowledge the financial support from the National Natural Science Foundation of China (No. 61671244, No. 61301108), and the Project of Jiangsu Provincial Six Talent Peaks (no.XYDXXJS-033).

References

[1] S. Timotheou and I. Krikidis, "Fairness for non-orthogonal multiple access in 5G systems," *IEEE Signal Processing Lett.*, vol. 22, no. 10, pp. 1647–1651, Oct. 2015.

[2] Y. Saito, Y. Kishiyama, A. Benjebbour, T. Nakamura, A. Li, and K. Higuchi, "Non-orthogonal multiple access (NOMA) for cellular future radio access," in *Proc. 2013 IEEE VTC Spring*, Jun. 2013, pp. 1–5.

[3] Q. Sun, S. Han, C. L. I, and Z. Pan, "On the ergodic capacity of MIMO NOMA systems," *IEEE Wireless Commun. Lett.*, vol. 4, no. 4, pp. 405–408, Aug. 2015.

[4] Z. Ding, P. Fan, and H. V. Poor, "Impact of user pairing on 5G nonorthogonal multiple-access downlink transmissions," *IEEE Tran. Veh. Tech.*, vol. 65, no. 8, pp. 6010–6023, Aug. 2016.

[5] C. Xue, Q. Zhang, Q. Li, and J. Qin, "Joint power allocation and relay beamforming in non-orthogonal multiple access amplify-and-forward relay networks," *IEEE Trans. Veh. Tech.*, vol. PP, no. 99, pp. 1–1, 2017.

[6] J. Choi, "Effective capacity of NOMA and a suboptimal power control policy with delay QoS," *IEEE Trans. Commun.*, vol. PP, no. 99, pp. 1–1, 2017.

[7] ——, "On the power allocation for a practical multiuser superposition scheme in NOMA systems," *IEEE Commun. Lett.*, vol. 20, no. 3, pp. 438–441, March 2016.

[8] B. Di, L. Song, and Y. Li, "Sub-channel assignment, power allocation, and user scheduling for non-orthogonal multiple access networks," *IEEE Trans. Wireless Commun.*, vol. 15, no. 11, pp. 7686–7698, Nov. 2016.

[9] L. Lei, D. Yuan, C. K. Ho, and S. Sun, "Power and channel allocation for non-orthogonal multiple access in 5G systems: Tractability and computation," *IEEE Trans. Wireless Commun.*, vol. 15, no. 12, pp. 8580–8594, Dec. 2016.

[10] Y. Sun, D. W. K. Ng, Z. Ding, and R. Schober, "Optimal joint power and subcarrier allocation for full-duplex multicarrier non-orthogonal multiple access systems," *IEEE Trans. Commun.*, vol. PP, no. 99, pp. 1–1, 2017.

[11] P. D. Diamantoulakis, K. N. Pappi, Z. Ding, and G. K. Karagiannidis, "Wireless-powered communications with non-orthogonal multiple access," *IEEE Trans. Wireless Commun.*, vol. 15, no. 12, pp. 8422–8436, Dec. 2016.

[12] H. Chingoska, Z. Hadzi-Velkov, I. Nikoloska, and N. Zlatanov, "Resource allocation in wireless powered communication networks with non-orthogonal multiple access," *IEEE Wireless Commun. Lett.*, vol. 5, no. 6, pp. 684–687, Dec. 2016.

[13] P. Diamantoulakis and G. Karagiannidis, "Maximizing proportional fairness in wireless powered communications," *IEEE Wireless Communications Letters*, vol. PP, no. 99, pp. 1–1, 2017.

[14] C. Xiong, L. Lu, and G. Y. Li, "Energy-efficient spectrum access in cognitive radios," *IEEE J. Sel. Areas Commun.*, vol. 32, no. 3, pp. 550–562, Mar. 2014.

[15] C. Shannon, "Communication theory of secrecy systems," *Bell Syst. Tech. J.*, vol. 28, no. 4, pp. 656–715, Oct. 1949.

[16] L. Ozarow and A. Wyner, *Wire-tap channel II Advances in Cryptology*. Berlin, Germany: Springer-Verlag, 1985.

[17] S. Karachontzitis, S. Timotheou, I. Krikidis, and K. Berberidis, "Security-aware max-min resource allocation in multiuser OFDMA downlink," *IEEE Trans. Information Forensics and Security*, vol. 10, no. 3, pp. 529–542, Mar. 2015.

[18] A. Kliks, O. Holland, A. Basaure, and M. Matinmikko, "Spectrum and license flexibility for 5G networks," *IEEE Comm. Mag.*, vol. 53, no. 7, pp. 42–49, Jul. 2015.

[19] A. Benjebbour, A. Li, K. Saito, Y. Saito, Y. Kishiyama, and T. Nakamura, "NOMA: From concept to standardization," in *Proc.2015 IEEE CSCN*, Oct. 2015, pp. 18–23.

[20] S. Wang, Z. H. Zhou, M. Ge, and C. Wang, "Resource allocation for heterogeneous cognitive radio networks with imperfect spectrum sensing," *IEEE J. Sel. Areas Commun.*, vol. 31, no. 3, pp. 464–475, Mar. 2013.

[21] Y. Zhang and C. Leung, "Resource allocation in an OFDM-based cognitive radio system," *IEEE Trans. Commun.*, vol. 57, no. 7, pp. 1928–1931, Jul. 2009.

[22] Z. Pan, Y. Zhang, and S. Kwong, "Efficient motion and disparity estimation optimization for low complexity multiview video coding," *IEEE Trans. Broadcasting*, vol. 61, no. 2, pp. 166–176, Jun. 2015.

[23] Z. Pan, J. Lei, Y. Zhang, X. Sun, and S. Kwong, "Fast motion estimation based on content property for low-complexity H.265/HEVC encoder," *IEEE Trans. Broadcasting*, vol. 62, no. 3, pp. 675–684, Sep. 2016.

[24] Z. Pan, P. Jin, J. Lei, Y. Zhang, X. Sun, and S. Kwong, "Fast reference frame selection based on content similarity for low complexity HEVC encoder," *IEEE Trans. Broadcasting*, vol. 40, no. B, pp. 516–524, Oct. 2016.

[25] C. Isheden and G. Fettweis, "Energy-efficient multi-carrier link adaptation with sum rate-dependent circuit power," in *Proc. 2010 IEEE GLOBECOM*, Dec. 2010, pp. 1–6.

[26] B. Tang, B. Ye, S. Lu, and S. Guo, "Coding-aware proportional-fair scheduling in OFDMA relay networks," *IEEE Trans. Parallel Distrib. Syst.*, vol. 24, no. 9, pp. 1727–1740, Sep. 2013.

[27] J. Willams and L. F., "A modification to the half-interval search (binary search) method," in *Proc. 1976 ACM Southeast Conference*, Apr. 1976, pp. 95–101.

[28] G. Auer, V. Giannini, C. Desset, I. Godor, P. Skillermark, M. Olsson, M. Imran, D. Sabella, M. Gonzalez, O. Blume, and A. Fehske, "How much energy is needed to run a wireless network?" *IEEE Wireless Commun.*, vol. 18, no. 5, pp. 40–49, Oct. 2011.

[29] A. G. Marques, L. M. Lopez-Ramos, G. B. Giannakis, and J. Ramos, "Resource allocation for interweave and underlay CRs under probability-of-interference constraints," *IEEE J. Sel. Areas Commun.*, vol. 30, no. 10, pp. 1922–1933, Nov. 2012.

[30] A. ParandehGheibi, A. Eryilmaz, A. Ozdaglar, and M. Medard, "On resource allocation in fading multiple-access channels an efficient approximate projection approach," *IEEE Trans. Information Theory*, vol. 56, no. 9, pp. 4417–4437, Sep. 2010.

[31] D. T. Ngo, S. Khakurel, and T. Le-Ngoc, "Joint subchannel assignment and power allocation for OFDMA femtocell networks," *IEEE Trans. Wireless Commun.*, vol. 13, no. 1, pp. 342–355, Jan. 2014.

[32] S. Boyd and L. Vandenberghe, *Convex Optimization*. Cambridge University Press, 2004.

[33] Q. Chen, G. Yu, R. Yin, and G. Y. Li, "Energy-efficient user association and resource allocation for multistream carrier

aggregation," *IEEE Trans. Veh. Technology*, vol. 65, no. 8, pp. 6366–6376, Aug. 2016.

[34] J. Papandriopoulos and J. S. Evans, "SCALE: A low-complexity distributed protocol for spectrum balancing in multiuser DSL networks," *IEEE Trans. Information Theory*, vol. 55, no. 8, pp. 3711–3724, Aug. 2009.

[35] T. Wang and L. Vandendorpe, "On the SCALE algorithm for multiuser multicarrier power spectrum management," *IEEE Trans. Signal Process.*, vol. 60, no. 9, pp. 4992–4998, Sep. 2012.

[36] N. Mokari, M. R. Javan, and K. Navaie, "Cross-layer resource allocation in OFDMA systems for heterogeneous traffic with imperfect CSI," *IEEE Trans. Veh. Technol.*, vol. 59, no. 2, pp. 1011–1017, Feb. 2010.